Research in Astronomy and Astrophysics, 24:015013 (5pp), 2024 January https://doi.org/10.1088/1674-4527/ad0a31

Study on the Performance of the GRANDProto300 Particle Detector Array by Simulation

Fu-Lin Dai[1,2,3], Quan-Bu Gou[3], Xiaoyuan Huang[1,2], and Yi-Qing Guo[3,4]
[1] Key Laboratory of Dark Matter and Space Astronomy, Purple Mountain Observatory, Chinese Academy of Sciences, Nanjing 210023, China; xyhuang@pmo.ac.cn
[2] School of Astronomy and Space Science, University of Science and Technology of China, Hefei 230026, China
[3] Key Laboratory of Particle Astrophysics, Institute of High Energy Physics, Chinese Academy of Sciences, Beijing 100049, China; gouqb@ihep.ac.cn
[4] University of Chinese Academy of Sciences, Beijing 100049, China
Received 2023 August 25; revised 2023 October 7; accepted 2023 October 25; published 2023 December 19

Abstract

The Giant Radio Array for Neutrino Detection (GRAND) is a proposed large-scale observatory designed to detect cosmic rays, gamma-rays, and neutrinos with energies exceeding 100 PeV. The GRANDProto300 experiment is proposed as the early stage of the GRAND project, consisting of a hybrid array of radio antennas and scintillator detectors. The latter, as a mature and traditional detector, is used to cross-check the nature of the candidate events selected from radio observations. In this study, we developed a simulation software called G4GRANDProto300, based on the Geant4 software package, to optimize the spacing of the scintillator detector array and to investigate its effective area. The analysis was conducted at various zenith angles under different detector spacings, including 300, 500, 600, 700, and 900 m. Our results indicate that, for large zenith angles used to search for cosmic-ray in the GRAND project, the optimized effective area is with a detector spacing of 500 m. The G4GRANDProto300 software that we developed could be used to further optimize the layout of the particle detector array in future work.

Key words: astroparticle physics – instrumentation: detectors – (ISM:) cosmic rays

1. Introduction

In 1912, Victor Hess detected a large excess of electrons in the upper atmosphere with a balloon experiment, which later was called cosmic radiation, and he won the Nobel Prize in Physics in 1936 for this work (Hess 1912). In 1958 and 1960, Kamata, Nishimura, and Greisen investigated the lateral distribution of the secondary particles from cosmic-ray air showers on the ground and proposed the Nishimura–Kamata–Greisen (NKG) function, which provides theoretical support for simulating and predicting experimental results (Kamata & Nishimura 1958; Greisen 1960). Physicists have been exploring and studying cosmic rays for over 100 yr since Hess' discovery. During this period, various experiments were developed to observe cosmic rays, including space satellites, ground-based, and underground experiments. Simulation software such as CORSIKA (Heck et al. 1998) and AIRES (Sciutto 1999) was also developed for studying air showers, which use different particle interaction models, such as GHEISHA (Maris et al. 2009) and ISOBAR (Deler & Valladas 1966) for low energy strong interaction models, and VENUS (Werner 1993), QGSJET (Ostapchenko 2011), SIBYLL (Ahn et al. 2009; Riehn et al. 2020), DPMJET (Ranft 1995), and HDPM (Knapp et al. 1997) for high energy strong interaction models. In order to search for even higher energy cosmic rays and solve the mysteries of their origins, new experiments are constantly being proposed. Among them, the Giant Radio Array for Neutrino Detection (GRAND) (Álvarez-Muñiz et al. 2020) is a hybrid array consisting of radio antennas (Huege 2016) and particle detectors. Particle detectors are widely used in various ground-based experiments, such as Tibet ASγ (Amenomori et al. 2008), LHAASO (Cao 2010), Telescope Array (TA) (Abu-Zayyad et al. 2012), Auger Prime (Abreu et al. 2012), LOFAR (Corstanje et al. 2015), and KASCADE-Grande (Apel et al. 2010). Since radio signals can be easily contaminated by other radio sources (Liu & Chen 2015), particle detectors could be used to cross-validate the results. This work mainly focuses on the perspective performance of the GRANDProto300 particle detector array, which is an early stage of the GRAND experiment, by simulation. To optimize its layout, we investigated the effective area of the particle detector array at different spacing configurations and zenith angles. We used CORSIKA to generate simulated cosmic-ray events, and to simulate the lateral distribution of secondary particles on the ground. We developed a detector simulation software called G4GRANDProto300 based on the Geant4 package to simulate the interaction between the detector and secondary particles. Finally, we performed a comparative analysis to optimize the particle detector array layout, aiming to maximize the effective area.

In Section 2 we present the GRANDProto300 experiment. In Section 3 we make a detailed introduction for the simulation software. In Section 4 we show the results. Finally, in Section 5 we present the conclusion.

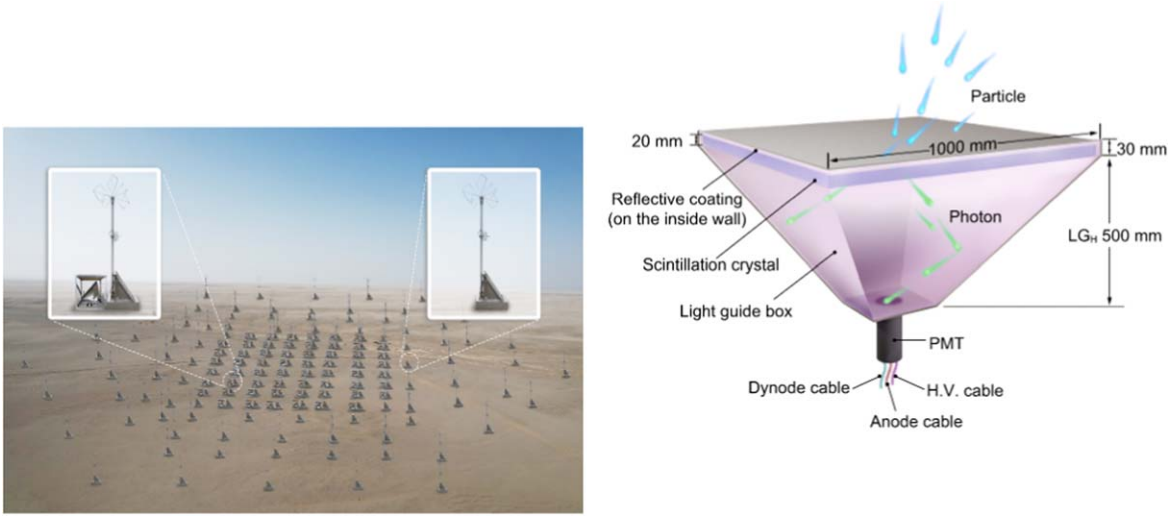

Figure 1. Schematic representation of the GRANDProto300 experiment (left) and the particle detector structure (right).

2. GRANDProto300 Experiment

The GRANDProto300 experiment is proposed as an early stage of the GRAND experiment, located on Xiaodushan in Dunhuang City, Gansu Province, China, at an altitude of 1300 m above sea level (Ma et al. 2023). This experiment is planned to consist of 300 radio antennas and 60 particle detectors, and some radio antennas have been deployed to test the data taking. The particle detector array is planned to be composed of 60 scintillator detectors, with 36 of them arranged in a 6×6 internal detector array and the remaining 24 arranged in a 4×6 guard ring. In the central area, the scintillator detector array and the antenna array of GRANDProto300 share the same layout and use the same electronics, allowing for a combined observation of the same event. The signals obtained with the scintillator detector array are synchronized with those obtained with the antenna array, enabling the simultaneous detection of the electromagnetic and muon components of the extensive air showers (EAS) (Pierog & Werner 2008).

The GRANDProto300 experiment is 10 times larger than the previous GRANDProto35 experiment (Gou et al. 2018), making it capable of observing primary cosmic rays exceeding 100 PeV. Currently, the GRANDProto300 particle detector array is in the simulation and optimization stage, while 13 out of 300 radio antennas are deployed on-site to start data taking (Ma et al. 2023). The experiment covers an area of 300 km^2 and is not sensitive enough for detecting neutrinos, but it is feasible for observing high-energy cosmic rays with large zenith angles. Figure 1 (left) shows the schematic layout of the GRANDProto300 experiment, which consists of an internal and an outer part. The internal part is made up of a back-to-back combination of particle detectors and radio antennas, whereas the outer part is made up of individual radio antennas. In the right panel of Figure 1, we show the designed structures, which would be used in the following simulation, for the particle detectors to collect electromagnetic and muon components of EAS.

3. Simulation Software

In this study, we utilized two simulation software packages. CORSIKA was used to simulate the air showers, while G4GRANDProto300, which is developed based on the Geant4 software package (Agostinelli et al. 2003; Allison et al. 2006), was used to simulate the interaction between the detector and secondary particles. By combining these two tools, we were able to simulate and analyze the performance of the array under different conditions and identify the optimal layout for the experiment. G4GRANDProto300 is developed with a structured, modular, and functional approach, including four directories, ten classes, and over 50 subroutines. Figure 2 provides a schematic representation of the G4GRANDProto300 software package.

The G4GRANDProto300 software mainly includes five modules:

1. *Parameter card control module* It controls the input parameters for the simulation. This module allows the user to specify various parameters, including the detector size information, which is crucial for constructing an accurate simulation of the particle detector array.
2. *Genbes module* It reads information about secondary particles produced by CORSIKA.
3. *Detector construction module* It constructs the detector structure and simulates the interactions between the particles and the detectors. Once the unit detector is constructed, it can be copied and arranged according to GRANDProto300's layout of the particle detectors, allowing for the construction of the entire array.

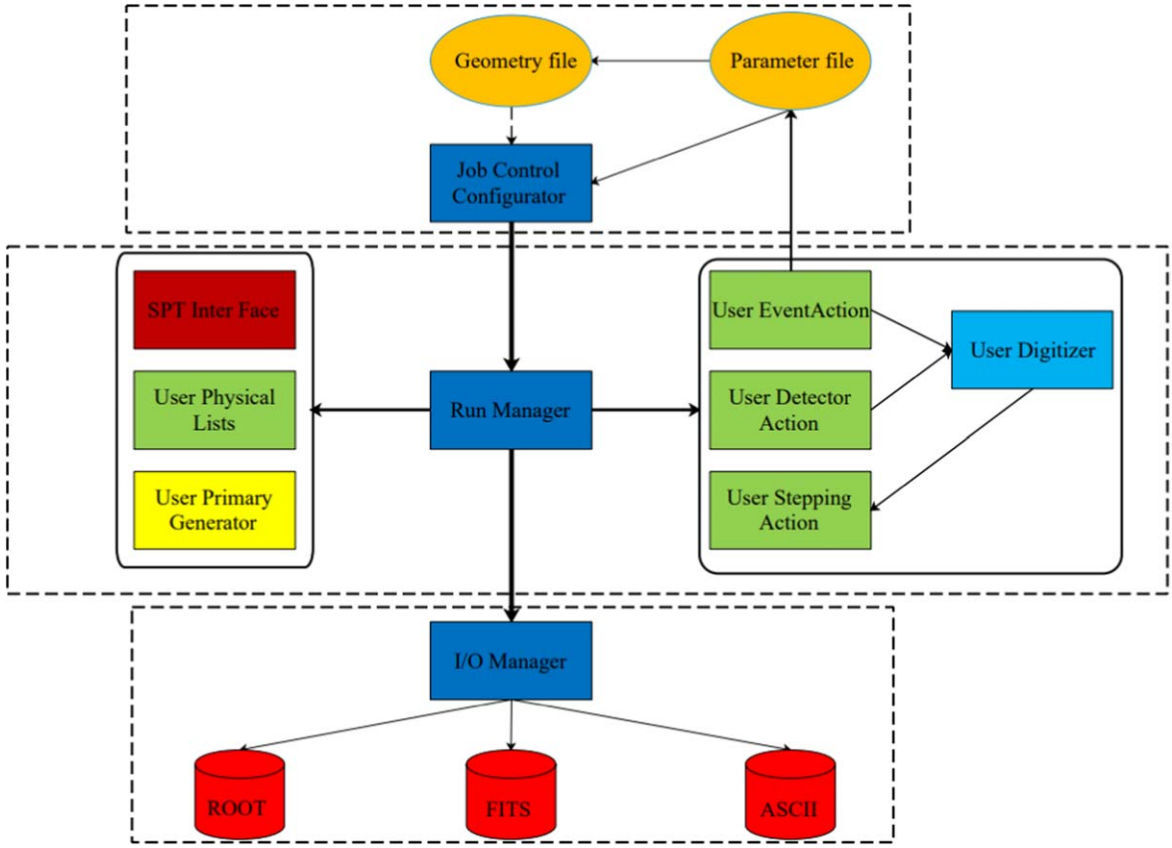

Figure 2. Schematic diagram of the GRANDProto300 detector simulation program.

4. *Digital module* It digitizes the signals from the detectors. In the digital process, realistic noises are added to the signal, according to the distribution of secondary cosmic-ray particles from the simulation. By accurately modeling the noise in the simulation, the digital module helps to ensure that the results from the simulation are realistic and can be compared to experimental data.
5. *Output module* It outputs the results of the simulation in various formats, including ROOT (Brun & Rademakers 1997), text, and FITS. The user can freely select the specific format they prefer and specify it in the parameter card. By providing multiple output formats, the output module allows for flexibility in data analysis and facilitates comparison with experimental data.

After running the simulation using the G4GRANDProto300 software package, the output data can be analyzed to obtain the expected performance of the array. By comparing the simulation results with experimental data, researchers can validate the accuracy of the simulation and gain a deeper understanding of the underlying physical processes. Furthermore, the analysis of the simulation output data could allow researchers to build the reconstruction pipeline, which is crucial for extracting meaningful information from detected cosmic-ray events.

4. Results

4.1. Detector Spacing Configuration

In the simulation, five sets of detector spacing were used, and a total of 180,000 events were generated in 20 batches for each detector spacing. The particle detector array for the GRANDProto300 experiment has different effective areas and sampling areas, depending on the spacing configuration. To balance the need for the computer resource for simulation and the area for the sampling area, we choose the sampling area large enough to cover the whole particle detector array, but not too large which could result in a large number of simulated events failing to trigger the detector. At a spacing of 300 m, the particle detector array has an area of 4.23 km^2 and a sampling area of 70.56 km^2. At a spacing of 500 m, the particle detector array area increases to 11.75 km^2 and the sampling area to 100 km^2. Similarly, at spacings of 600, 700, and 900 m, the particle detector array areas are 16.92 km^2, 23.03 km^2, and 38.07 km^2, respectively, while the sampling areas are 121, 219.04, and 219.04 km^2.

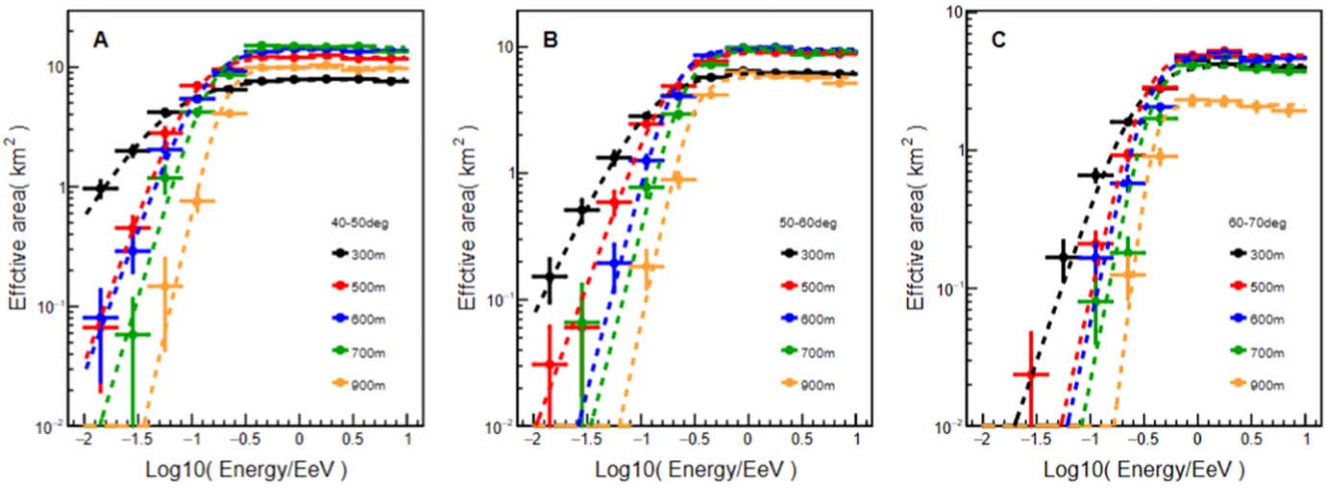

Figure 3. The effective area of the particle detector array with different spacing under 3 different zenith angle bins.

4.2. Effective Area

The effective area of the particle detector array can be calculated using the formula Equation (1):

$$A_{\text{eff}} = \frac{n}{N} \cdot A_s \cdot \cos\theta \tag{1}$$

where n is the number of cosmic ray events observed, with at least 4 detectors triggered, by the particle detector array, N is the number of cosmic ray events assumed in the simulation, A_s is the sampling area, and θ is the zenith angle of the cosmic ray. To assess the reliability of the results and determine the statistical significance of any observed effects, the error bar of the effective area of the particle detector array (ΔA) can be calculated using the formula Equation (2):

$$\Delta A = \frac{\sqrt{n}}{N} \cdot A_s \cdot \cos\theta. \tag{2}$$

The investigation was conducted at three different zenith angle bins (40°–50°, 50°–60°, and 60°–70°), with five different detector spacings (300, 500, 600, 700, and 900 m). Figure 3 displays the effective area of the particle detector array for different detector spacings under three different zenith angle intervals. The effective area of the particle detector array regularly increases with energy and reaches a plateau, regardless of the different zenith angles or detector spacing. The flat behavior of the effective area in the plateau indicates that the particle detector array reaches its full efficiency for cosmic rays in this energy region. To describe the curve, an equation similar to the Sigmoid function was adopted. The equation is expressed as Equation (3):

$$A = A_p \cdot \frac{1}{1 + \exp\left(-\frac{E - p_1}{p_2}\right)} \tag{3}$$

where A_p is the effective area to reach the plateau, p_1 is the primary cosmic ray energy corresponding to the initial arrival at the plateau, and p_2 is the parameter that controls the shape of the curve of the function and affects the rate at which the slope changes. Using this equation for fitting, the obtained Chi2/Ndf values are not greater than 2.

For the large zenith angle bins of 60°–70°, according to the analysis, the effective area (A_p) and the energy at which the platform is reached vary depending on the spacing of the detector array. Here are the results:

·For a 300 m spaced detector array: $A_p = 4.15$ km^2, platform energy = 272.54 PeV.

·For a 500 m spaced detector array: $A_p = 4.90$ km^2, platform energy = 322.24 PeV.

·For a 600 m spaced detector array: $A_p = 4.75$ km^2, platform energy = 355.44 PeV.

·For a 700 m spaced detector array: $A_p = 4.11$ km^2, platform energy = 376.44 PeV.

·For a 900 m spaced detector array: $A_p = 2.14$ km^2, platform energy = 390.28 PeV.

These results indicate that the 500 m spaced detector array yields the largest effective area (4.90 km^2) and reaches the platform at moderate energy (322.24 PeV).

The weighted effective area (A_{weighted}) can also be utilized to study the detector configuration. It can be calculated using the formula Equation (4):

$$A_{\text{weighted}} = \sum_i w_i \cdot A_p^i \tag{4}$$

where w_i denotes the weight at different zenith angles, and A_p^i is the effective area of the same detection array at different zenith angles. The weight can be set according to the purpose of the experiment. But as a simple example, we simply set w_i as 1 for one desired zenith angle and set it as 0 for other 2 zenith angles, as shown in Figure 4 for the weighted effective area at

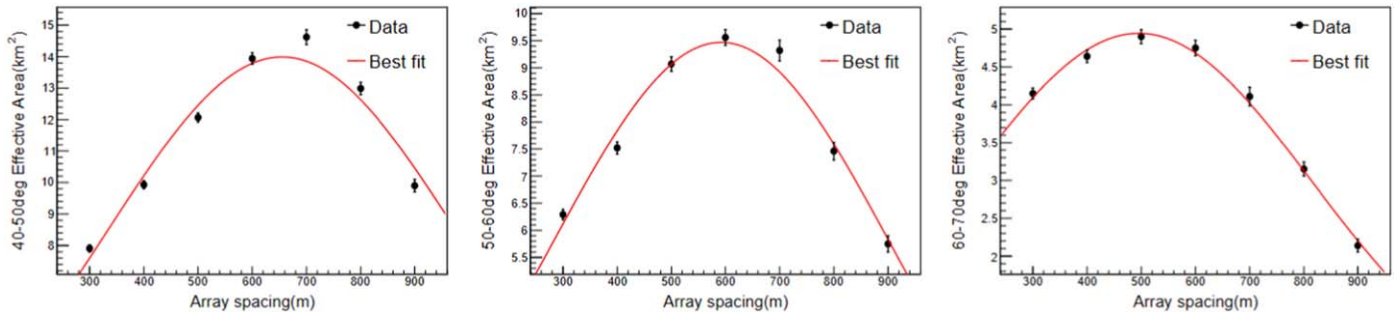

Figure 4. Effective area at different spacing configurations under different zenith angle bins (40°–50°, 50°–60°, 60°–70° from left to right).

different spacing configurations under different zenith angle bins. We fit the effective area as a function of spacing using a Gaussian function. As can be clearly seen from Figure 4, at zenith angles of 40°–50°, the detector array with a spacing of 654.9 ± 3.74 m exhibits the largest effective area. Within the 50°–60° range, the effective area is maximized for a spacing of 592.2 ± 3.63 m. As the zenith angle increases, the detector layout with a spacing of 495.5 ± 6.12 m achieves the largest effective area at large zenith angles of 60°–70°. It is evident that as the zenith angle increases, the range of maximum effective area shifts toward smaller spacing intervals. For cosmic rays at large zenith angles, the increased atmospheric thickness leads to a decrease in lateral particle density at greater distances from the shower axis, making detection difficult for larger spacing configurations.

For the large zenith angle bins of 60°–70°, the weight was set to 1, and a Gaussian fit was conducted to determine the optimal spacing value of 495.5 ± 6.12 m and the peak effective area value of 4.94 ± 0.06 km^2. This means that under a large zenith angle, a detector spacing of 500 m can be selected to obtain a larger effective area, thereby improving the detection ability of the experiment.

5. Conclusion

The G4GRANDProto300 software is developed based on the widely-used Geant4 software package, which is commonly used for detector simulations and can also be used to simulate the triggering of cosmic rays, incorporating the design for the particle detector of GRANDProto300. We used this program to study the effect of different detector spacing on the effective area under different zenith angles. The spacing was set to 300, 500, 600, 700, and 900 m, at zenith angle bins of 40°–50°, 50°–60°, and 60°–70° for incident cosmic-ray. We found that for large zenith angles, a detector spacing of 500 m provides a better effective area compared to other spacing options for the detector array. By comparing the simulation results with the experimental data of a detector unit, we verified the reliability of this software, which provides solid support for the performance simulation of the GRANDProto300 particle detector array. The G4GRANDProto300 simulation software developed in this work can also provide strong support for the layout study of other particle detector arrays in the future.

Acknowledgments

The work presented here does not necessarily represent the views of the GRAND Collaboration. This work is supported by the National Natural Science Foundation of China (Nos. 12 322 302, 12 275 279 and U1931201), the National Key R&D Program of China (No. 2023YFE0102300), the Project for Young Scientists in Basic Research of Chinese Academy of Sciences (No. YSBR-061), and the Chinese Academy of Sciences, and the Entrepreneurship and Innovation Program of Jiangsu Province.

References

Abreu, P., Aglietta, M., Ahlers, M., et al. 2012, JINST, 7, P10011
Abu-Zayyad, T., Aida, R., Allen, M., et al. 2012, NIMPA, 689, 87
Agostinelli, S., Allison, J., Amako, K., et al. 2003, NIMPA, 506, 250
Ahn, E.-J., Engel, R., Gaisser, T. K., Lipari, P., & Stanev, T. 2009, PhRvD, 80, 094003
Allison, J., Amako, K., Apostolakis, J., et al. 2006, ITNS, 53, 270
Álvarez-Muñiz, J., Alves Batista, R., Balagopal, V. A., et al. 2020, SCPMA, 63, 219501
Amenomori, M., Bi, X. J., Chen, D., et al. 2008, JPhCS, 120, 062024
Apel, W. D., Arteaga, J. C., Badea, A. F., et al. 2010, NIMPA, 620, 202
Brun, R., & Rademakers, F. 1997, NIMPA, 389, 81
Cao, Z. 2010, ChPhC, 34, 249
Corstanje, A., Schellart, P., Nelles, A., et al. 2015, APh, 61, 22
Deler, B., & Valladas, G. 1966, NCimA, 45, 559
Gou, Q., Martineau-Huynh, O., David, J., et al. 2018, PoS, ICRC2017, 388
Greisen, K. 1960, ARNPS, 10, 63
Heck, D., Knapp, J., Capdevielle, J. N., Schatz, G., & Thouw, T. 1998,
Hess, V. F. 1912, PhyZ, 13, 1084
Huege, T. 2016, PhR, 620, 1
Kamata, K., & Nishimura, J. 1958, PThPS, 6, 93
Knapp, J., Heck, D., & Schatz, G. 1997, NuPhS, 52, 136
Liu, W., & Chen, X. 2015, RAA, 15, 623
Ma, P.-X., Duan, B.-H., Xu, X., et al. 2023, PoS, ICRC2023, 304
Maris, I. C., Engel, R., Garrido, X., et al. 2009, NuPhS, 196, 86
Ostapchenko, S. 2011, PhRvD, 83, 014018
Pierog, T., & Werner, K. 2008, PhRvL, 101, 171101
Ranft, J. 1995, PhRvD, 51, 64
Riehn, F., Engel, R., Fedynitch, A., Gaisser, T. K., & Stanev, T. 2020, PhRvD, 102, 063002
Sciutto, S. J. 1999, arXiv:astro-ph/9911331
Werner, K. 1993, PhR, 232, 87